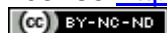




Article (refereed) - postprint

Wang, Wei; Liu, Xuejun; Xu, Jin; Dore, Anthony J.; Xu, Wen. 2018.
Imbalanced nitrogen and phosphorus deposition in the urban and forest environments in southeast Tibet.

© 2018 Turkish National Committee for Air Pollution Research and Control.
This manuscript version is made available under the CC-BY-NC-ND 4.0
license <http://creativecommons.org/licenses/by-nc-nd/4.0/>



This version available <http://nora.nerc.ac.uk/519716/>

NERC has developed NORA to enable users to access research outputs wholly or partially funded by NERC. Copyright and other rights for material on this site are retained by the rights owners. Users should read the terms and conditions of use of this material at <http://nora.nerc.ac.uk/policies.html#access>

NOTICE: this is the author's version of a work that was accepted for publication in *Atmospheric Pollution Research*. Changes resulting from the publishing process, such as peer review, editing, corrections, structural formatting, and other quality control mechanisms may not be reflected in this document. Changes may have been made to this work since it was submitted for publication. A definitive version was subsequently published in *Atmospheric Pollution Research* (2018), 9 (4). 774-782.

<https://doi.org/10.1016/j.apr.2018.02.002>

www.elsevier.com/

Contact CEH NORA team at
noraceh@ceh.ac.uk

1 **Imbalanced nitrogen and phosphorus deposition in the urban and forest**
2 **environments in southeast Tibet**

3 Wei Wang ^{1,2}, Xuejun Liu ², Jin Xu ¹, Wen Xu ^{3,4*}

4 1. Xizang Agriculture and Animal Husbandry College, Nyingchi, Tibet, 860000, China

5 2. College of Resources and Environmental Sciences, China Agricultural University, Beijing
6 100193.

7 3. State Key Laboratory of Urban and Regional Ecology, Research Center for Eco-Environmental
8 Sciences, Chinese Academy of Sciences, Beijing 100085, China

9 4. College of Resources and Environment, University of Chinese Academy of Sciences, Beijing
10 100049, China.

11 * Corresponding author (E-mail: hi.xuwen@163.com)

12 **Abstract:** In the last decades, in China a large amount of anthropogenic emissions has
13 dramatically increased nitrogen (N) deposition and may lead to an imbalance of
14 atmospheric N and phosphorus (P) inputs in terrestrial ecosystems. However, the
15 status of N and P deposition in southeast Tibet is poorly understood. Here, we
16 investigated spatial and monthly patterns of N and P deposition based on
17 measurements of dissolved inorganic N (DIN, including ammonium N and nitrate N)
18 and dissolved organic N (DON) and total dissolved P (TDP) in precipitation from
19 March to October 2017 at an urban site in Nyingchi (NC) city and at a forest site in
20 Sejila (SJL) Mountain. Over the study period, monthly total dissolved N (sum of DIN
21 and DON) deposition fluxes summed 4.6 and 3.6 kg N ha⁻¹ at SJL and NC per year,
22 respectively, of which dissolved organic nitrogen accounted for 35% and 38%.
23 Monthly averages showed an increase trend from March to June, and then decrease in
24 autumn months (September and October). At both two sites, ratios of ammonium to
25 nitrate N in bulk deposition are greater than 1, indicating reduced N mainly from
26 agricultural sources dominated N deposition in study area. Monthly TDP deposition
27 fluxes summed to 0.68 and 0.58 kg P ha⁻¹ per year at SJL and NC, respectively, both
28 of which showed an increased trend from March to May and decreased trend from
29 July to October. The N/P ratio was 6.1 and 6.8 at NC and SJL, respectively.

30 **Keyword:** Nitrogen deposition; Phosphorus deposition; N/P ratio; Dissolved organic

31 nitrogen deposition; Tibet Plateau

32 **1. Introduction**

33 Nitrogen (N) and phosphorus (P) are essential elements for plant growth in
34 terrestrial and marine ecosystems, but can also be considered as limiting elements
35 when their supply does not meet demands by microbes and plants (Elser et al., 2007).
36 Over the past few decades, reactive N (Nr) and P levels in the atmosphere have been
37 increased significantly due to rapid development of industrialization and agricultural
38 production, resulting in substantial increases in atmospheric N and P deposition to
39 terrestrial ecosystems (Smil, 2000; Galloway et al., 2004; Liu et al., 2013). It has been
40 estimated that at a global scale, anthropogenic Nr inputs to the biosphere were
41 between 165–259 M ton N yr⁻¹ globally, N deposition fluxes were about 114 M ton N
42 yr⁻¹ in the year 2000 and is expected to be a upward trend in the future (Peñuelas et al.
43 2012). In contrast, anthropogenic P inputs to biosphere were 22-26 M ton N yr⁻¹, and
44 global P deposition were 3-4 M ton N yr⁻¹ since 1980 but had no obvious temporal
45 trend (Peñuelas et al. 2013).

46 Due to the negative effects from excessive deposition on the environment, many
47 studies have quantified magnitudes of N and/or P deposition at regional or national
48 scales and differentiate their chemical compositions, especially N deposition (Lü et al.,
49 2007; Duce et al., 2008; Jia et al., 2014; Lu et al., 2014; Zhu et al., 2015 Liang et al.,
50 2016). For example, based on 5-year field measurements, Xu et al. (2015) reported
51 that total N deposition (wet and dry) ranged from 2.9 kg N ha⁻¹ yr⁻¹ to 83.8 kg N ha⁻¹
52 yr⁻¹ at 43 *in situ* monitoring sites across China. However, only few monitoring reports
53 on atmosphere P deposition exist and are limited to particulate P (Luo et al., 2011;
54 Parron et al., 2011; Hou et al., 2012; Du et al., 2016). It is well known that a complete
55 quantification of P deposition is a big challenge, since P has no stable gaseous phase
56 in the atmosphere and is mainly spread by wind in form of dust (Smil, 2000;
57 Mahowald et al., 2008). At a national scale, Zhu at al. (2016) reported that wet P
58 deposition ranged from 0.093 to 0.63 kg P ha⁻¹ yr⁻¹ at 41 *in situ* field stations across
59 China. Their results also show that the ration of N to P in wet deposition was 77 (by

60 mass), much higher than N:P ratios (~47, based on molar) of global N deposition in
61 continents and/ or those of terrestrial plants (22-30, based on molar) (Peñuelas et al.,
62 2013).

63 The Qinghai-Tibet plateau, occupying about one-fourth of the land area of China
64 (Zhang et al., 2002), is sensitive to global climate change (Liu et al., 2013; Xu et al.,
65 2014). Long-term N addition can decrease the species richness of both vegetation and
66 soil seed banks in alpine meadow ecosystems (Ma et al., 2014). At present, little is
67 known about magnitude of N deposition in Qinghai-Tibet plateau (Liu et al., 2015;
68 Zhu et al., 2015). In addition, atmospheric P deposition in the Qinghai-Tibet plateau
69 remains unclear, especially in southeast Tibet, which accounted for 80% of the total
70 forest area (1.47×10^7 ha) in Tibet Province. In this paper, we presented estimates of
71 bulk N and P deposition at two field monitoring sites in Nyingchi (NC) city and Sejila
72 (SJL) mountain during the main rain season from March to October 2017, with the
73 purposes being to quantify fluxes, forms and monthly variations of N and P deposition
74 (as precipitation with continuously-open collector) to better understanding the current
75 status of N and P deposition and impacts in remote region of China.

76 **2. Materials and methods**

77 **2.1 Site description**

78 For bulk N and P deposition measurements, the monitoring site in NC city was
79 located at Xizang Agriculture and Animal Husbandry College (29°66'N 94°34'E 2990
80 m a.g.l.), southeast of the city, whereas that in SJL mountain was established at the
81 National Field Scientific Observation Station of Alpine Forest Ecosystem (29°65'N
82 94°72'E 3950 m a.g.l.), on the edge of the NC city (**Fig. 1**). Nyingchi City is located
83 beside the Niyang River, which was one of the main tributaries of the Brahmaputra.
84 The climate is mainly dominated by warm air currents in the Indian Ocean, with an
85 annual average temperature of 8.7°C and an annual average precipitation of 650 mm.
86 Tourism is a major local economic pillar industry. At NC site, there was no heavy
87 industry nearby, and potential emission sources were a small village and agricultural
88 fields. The SJL site was surrounded by original fir forest, in which undergrowth

89 vegetation were mainly *Sorbus*, *Rosa*, *Lonicera* and some other herbaceous plant. At
90 this site, there were no anthropogenic Nr emission sources except for a state road
91 (#318). Annual average temperature was -0.73°C and annual average precipitation
92 was about 1000 mm.

93 **2.2 Sampling and chemical analysis**

94 The rainwater samples were collected by continuously-open rain gauge, and thus
95 contain mainly wet and unquantifiable fractions from gaseous and particulate Nr in
96 dry-deposited process. In other word, wet deposition measured in the present work is
97 actually bulk deposition. Rain gauge consists of a stainless steel funnel and glass
98 bottle and was installed 1.2 m above the ground. After each precipitation event, the
99 rainwater samples were thoroughly stirred and immediately stored in clean
100 polyethylene bottles (50 ml), and then, the rainwater-collecting bottle was rinsed with
101 deionized water to eliminate cross contamination. All samples were filtered with a
102 0.45 mm syringe filter (Tengda Inc., Tianjin, China), then filtrates were frozen in a
103 refrigerator at -20°C until prior to analysis in the laboratory.

104 The laboratory analysis was performed according to Chinese standard methods.
105 Total dissolved nitrogen (TDN) was measured by alkaline potassium persulfate
106 digestion-UV spectrophotometric method (GB11894-89); Nitrate nitrogen (NO_3^- -N)
107 was measured by UV spectrophotometric Method; ammonium nitrogen (NH_4^+ -N) was
108 measured by reagent colorimetric method (GB7479-87); Total dissolved phosphorus
109 (TDP) was measured by ammonium molybdate spectrophotometric method
110 (GB11893-89); Rainwater was digested using intelligent multiparameter digestion
111 meter (LH-25A, Lianhua, China). NO_3^- -N, NH_4^+ -N, and TDP were measured using
112 ultraviolet and visible spectrophotometer (DR6000, HACH, America). DON
113 concentration was defined as the difference between the TDN and inorganic N
114 (NH_4^+ -N and NO_3^- -N) concentrations (Zhang et al., 2012). During each analysis,
115 rainwater samples were analyzed in duplicates and each analysis run consisted of 8
116 samples, one blank and a set of standard concentrations of NH_4^+ -N, NO_3^- -N and TDN.
117 Standard solutions were prepared in deionized water with concentrations ranges both
118 $0\text{-}1\text{ mg L}^{-1}$ for NH_4^+ -N and NO_3^- -N, and $0\text{-}2\text{ mg L}^{-1}$ for TDN. TDP contains phosphate

119 and dissolved organic P. Duplicate blank and standard reference materials
120 (monopotassium phosphate, KH_2PO_4) methods were used for quality assurance.

121 **2.3 Data calculation and analysis**

122 Monthly Nr (TDN, $\text{NH}_4^+\text{-N}$, $\text{NO}_3^-\text{-N}$, DON) bulk deposition fluxes were
123 calculated as follows:

$$124 \quad N = \sum_{i=1}^n Ni * Pi / 100$$

125 Monthly dissolved phosphorus deposition fluxes were calculated as follows:

$$126 \quad D = \sum_{i=1}^n Di * Pi / 100$$

127 where P is the precipitation per month(mm); N is bulk deposition fluxes of
128 measured Nr species (TDN, $\text{NH}_4^+\text{-N}$, $\text{NO}_3^-\text{-N}$) ($\text{kg ha}^{-1} \text{ month}^{-1}$); D is the total
129 dissolved phosphorus deposition fluxes ($\text{kg ha}^{-1} \text{ month}^{-1}$); *i* is the number of
130 precipitations per month; *Pi* is the precipitation volume in *i* precipitation events; *Ni* is
131 the volume-weighted mean concentration of measured Nr (TDN, $\text{NH}_4^+\text{-N}$, $\text{NO}_3^-\text{-N}$)
132 components in *i* precipitation events; *Di* is the is the volume-weighted mean
133 concentration of TDP in *i* precipitation events; 100 is the unit conversion factor of
134 mgm^{-2} to kgha^{-1} .

135 **2.4 Statistical analysis**

136 Pearson correlation and regression analyses were conducted using the SPSS
137 software package, version 20.0 (SPSS Inc., Chicago, IL), and significance was tested
138 using a significance level (*P*) of 0.05.

139 **2.5 Backward trajectory analysis**

140 To recognize the potential sources and transport routes of air pollutants and
141 precipitation clouds, air mass backward trajectory analysis was performed using the
142 Hybrid-Single Particle Integrated Trajectory Model (HYSPLIT 4) (Xu et al., 2017),
143 provided by the Air Resource Laboratory of National Oceanic and Atmospheric
144 Administration (NOAA) (Stein et al., 2015; Roy et al., 2016). Meteorological data
145 were input from the Global Data Assimilation System (GDAS) meteorological data
146 archives of the Air Resource Laboratory, National Oceanic and Atmospheric
147 Administration (NOAA). Three-day backward trajectories were calculated at 6 h

148 intervals (00:00, 06:00, 12:00, 18:00 UTC) on sampling days at both two study sites,
149 with arrival height of 500 m above ground level. Then, cluster analysis was performed
150 using the trajectories based on the total spatial variance (TSV) method (Draxler et al.,
151 2012).

152 3. Results

153 3.1 Concentrations of Nr species and TDP in precipitation

154 Total rainfall amounts during March-October, the main rain season were 624.8
155 mm at NC and 838.3mm at SJL. Monthly precipitation amounts at SJL were higher
156 than those at LZ city in all months except March and September (Fig. 2a). As showed
157 in Fig. 3, total volume-weighted mean concentrations of $\text{NH}_4^+\text{-N}$ were slightly higher
158 than those of $\text{NO}_3^-\text{-N}$ at both monitoring sites (0.19 versus 0.17 mg/L at SJL, and 0.22
159 versus 0.13 kg N ha⁻¹ at NC). In general, concentration of $\text{NH}_4^+\text{-N}$, DON, TDN and
160 TDP at NC were all higher than those at SJL, but opposite behavior occurred for
161 $\text{NO}_3^-\text{-N}$.

162 3.2 Atmosphere bulk deposition of Nr species and TDP

163 During the study period, monthly bulk deposition fluxes of $\text{NO}_3^-\text{-N}$, $\text{NH}_4^+\text{-N}$ and
164 DON were in the ranges of 0.01-0.23, 0.02-0.32, and 0.02-0.30 kg N ha⁻¹ at NC,
165 respectively, whereas those were in the ranges of 0.02-0.35, 0.02-0.42, 0.02-0.47 kg N
166 ha⁻¹ at SJL (Figs. 2d-f). At both two sites, bulk $\text{NO}_3^-\text{-N}$, $\text{NH}_4^+\text{-N}$ and DON deposition
167 fluxes generally show an increasing trend from March to June, and decrease trend
168 from August to October. Compared with SJL, bulk deposition fluxes of $\text{NO}_3^-\text{-N}$ at NC
169 were lower in all months. Differently, bulk $\text{NH}_4^+\text{-N}$ deposition fluxes were higher in
170 March, May, September and October, bulk DON deposition fluxes were higher in July
171 and September, but lower in other months. In total, bulk TDN deposition fluxes at NC
172 were lower than those at SJL in all months except September (Fig. 2b). At each site,
173 bulk TDN deposition fluxes showed a significant and positive correlation with
174 precipitation amounts (Fig. 4a).

175 Monthly TDP deposition ranged from 0.01 to 0.16 kg ha⁻¹ at SJL, and from 0.01
176 to 0.14 kg P ha⁻¹ at NC (Fig. 2c), with an increasing trend from March to May, and a

177 decreasing trend from Jul to October. The TDP deposition fluxes at SJL were higher
178 than those at NC in all months except April and September. A positive linear
179 relationship was found between TDP deposition fluxes and precipitation amounts at
180 both two sites (**Fig. 4b**).

181 Based on monthly averages in the main rainy season, bulk deposition fluxes of
182 TDN at SJL and NC summed 4.62 and 3.57 kg N ha⁻¹, respectively, with contributions
183 of 34% and 38% from DON. Bulk deposition fluxes of TDP summed 0.68 and 0.58 kg
184 P ha⁻¹ at SJL and NC, respectively. (**Fig. 5**). The N/P ratio was 6.76 and 6.11 at SJL
185 and NC, respectively.

186 **4. Discussion**

187 A large variability in the monthly volume-weighted mean concentrations of Nr
188 species (NH₄⁺-N, NO₃⁻-N, and DON) and TDP in bulk precipitation was found at both
189 study sites. The lowest concentrations in bulk precipitation are associated with the
190 highest precipitation rates during summer months ([Pineda Rojas and Venegas, 2010](#)).
191 This can be explained because the first drops of rainfall perform an intense
192 atmospheric N and P scavenging, which increases the rainwater N and P concentration
193 in low rainfall events ([Al-Khashman, 2009](#); [Zhang et al., 2012](#); [Sun et al., 2014](#)). We
194 observed that NH₄⁺-N and NO₃⁻-N concentrations in bulk precipitation are positively
195 well correlated at the NC site (R²=0.31, P<0.05) (**Fig. 6a**), suggesting the existence of
196 dissolved NH₄NO₃ in precipitation from the atmosphere ([Bertollini et al., 2016](#)). The
197 presence of NH₄NO₃ in precipitation is related to volatilized fertilizers which have
198 been dissolved in rain droplets and deposited in rainfall events ([Niu et al., 2014](#)). The
199 relationships between DON and NO₃⁻-N, and DON and NH₄⁺-N concentrations at NC
200 were negative and statistically significant and were correlated by fitting a logarithmic
201 model (**Figs. 6b and c**). These results indicate similar origins of atmospheric organic
202 and inorganic N compounds in bulk deposition at NC sites. In contrast, the
203 correlations between NH₄⁺-N, NO₃⁻-N and DON were all not statistically significant
204 (P>0.05) at SJL. A non-significant correlation was also reported by several other
205 previous studies ([Neff et al., 2002](#); [Yang et al., 2010](#)). The different chemical

206 composition correlations between the NC and SJL sites is likely linked with the
207 differences in wet scavenging (in-cloud and below-cloud) of gases and particles and
208 sources of DON, which can affect concentrations of inorganic and organic N_r species
209 in precipitation (Seinfeld and Pandis, 1998; Yang et al., 2010).

210 Bulk N deposition is influenced by several factors, such as precipitation amounts
211 and the seasonal variability of emission sources as well as N removal from the
212 atmosphere via chemical and physical processes (Yu et al., 2011; Kuang et al., 2016;
213 Liu et al., 2016; Calvo-Fernández et al., 2017; Xing et al., 2017; Xu et al., 2018). The
214 present results show that precipitation amounts varies greatly between different
215 months at the two study sites, with higher levels in May, June, July, and August (**Fig.**
216 **2a**). Higher bulk N and TDP deposition fluxes were also found corresponding to
217 those months (**Fig. 2b,c**). We also observed relatively high NO₃⁻-N deposition fluxes
218 in June and September at SJL. Not surprisingly, a high deposition level was observed
219 in September when precipitation amounts were relatively small. Diesel generators, a
220 major NO_x emission source (Liu et al., 2011), were frequently used for construction
221 and reconstruction works carrying out only in September at SJL. Thus, an elevated
222 atmospheric NO_x level resulting from large amounts of NO_x emissions from Diesel
223 generators is a likely explanation for high NO₃⁻-N deposition fluxes. Estimated
224 NH₄⁺-N deposition fluxes were higher in May at NC, which is likely due to the
225 increased volatilization of NH₃ from local agricultural activities (cultivation and
226 fertilization) in April and May caused by higher temperatures (Xu et al., 2014).

227 DON categories mainly include reduced organic nitrogen, oxidized organic
228 nitrogen and biological organic nitrogen (Graedel et al., 1986). It has been reported
229 that the averaged DON deposition flux was 6.84 kg N ha⁻¹ yr⁻¹, and accounted for
230 more than 50% of total N deposition fluxes in a forest ecosystem (Zhang et al., 2012).
231 A similar phenomenon was also observed in the present work. DON deposition fluxes
232 were extremely high in June at SJL, mainly due to relatively high pollen grain
233 sedimentation in summer (Bovallius et al., 1978). Similarly monthly TDP deposition
234 fluxes were higher during May-July compared to other months at both monitoring site,
235 especially at SJL (**Fig. 4**). This can be attributed to the fact that atmosphere

236 pollen grain sedimentation is the major source of atmospheric P deposition
237 (Mahowald et al. 2008). It has been estimated that the phosphorus content was about
238 0.5% in *Euphoria longan* pollen grain (Liu et al., 1995). SJL Mountain, the selected
239 monitoring site was located in a clearing surrounded by plants like *Abies georgei*,
240 *Sorbus rehderiana*, *Rosa multiflora*, all of which flowered during May-late July every
241 year, thus lead to relatively higher bulk TDP deposition.

242 For the Qinghai-Tibet plateau, bulk N deposition fluxes averaged 7.62 ± 8.60 kg
243 N ha⁻¹ yr⁻¹ at two urban and forest sites (Xu et al., 2015) **Error! Bookmark not**
244 **defined.** Wet N deposition levels ranged from 0.44 to 1.55 kg N ha⁻¹ yr⁻¹ for
245 inorganic N at 5 remote sites (Liu et al., 2015), with 8.36 ± 4.19 kg N ha⁻¹ yr⁻¹
246 estimated for total dissolved N deposition at a regional scale (Zhu et al., 2016). These
247 results imply the existence of large spatial variability in wet/bulk N deposition in the
248 Tibet plateau. By contrast, bulk TDN deposition fluxes we measured were 4.62 and
249 3.57 kg N ha⁻¹ at SJL and NC, respectively. According to the China Meteorological
250 Data Network statistics (<http://data.cma.cn/data/weatherBk.html>), the average
251 precipitation amount from November to February was 11.4mm during the last 30
252 years (1981-2010) next year in NC city, accounting for 1.6% of the annual
253 precipitation amount. Given such relatively low precipitation from October to
254 February, the fluxes measured during March-October at NC and SJC can reflect their
255 respective annual deposition levels to some extent. Similar research has reported that
256 average total dissolved N deposition was 7.9 kg N ha⁻¹ yr⁻¹ during 2012-2013 in a
257 southeast forest ecosystem (Liu et al., 2016). It is commonly accepted that N and P
258 deposition have been enhanced by human activities (Peñuelas et al. 2012; Peñuelas et
259 al., 2013). However, bulk N deposition fluxes were higher at SJL compared with
260 those at NC (Fig. 5), although the former is considered to be a remote forest
261 monitoring site. This is mainly due to higher precipitation amounts at SJL than at NC
262 (Fig. 2a), since bulk N deposition fluxes were influenced not only by rainfall Nr
263 concentration but also by precipitation amounts (Xu et al., 2015) Compared with other
264 Nr species, bulk NO₃⁻-N deposition fluxes differed clearly between SJL and NC (Fig.
265 3). One explanation is that SJL mountain monitoring site is located near State Road

266 (#318) (which is a major road in Tibet), and thus was polluted by NO_x emissions from
267 fossil fuel combustion in transportation (Liu et al. 2011). It should be pointed out that
268 bulk deposition is used here to refer to wet plus part of the dry deposition collected by
269 rain gauges that remain open to the atmosphere. Based on a full two-year (2014-2015)
270 measurements of monthly NO_2 and NH_3 concentration at a suburban site in Xining
271 City, Qinghai Province, Xu et al. (2017b) found that dry N deposition accounted for
272 46% of the total deposited N. This highlights the importance of dry deposition in the
273 urban environment, even in remote area of China. Thus, to assess the influence from
274 dry deposition, a comparison of mean bulk deposition and wet-only deposition at two
275 study sites is recommended in future studies.

276 The $\text{NH}_4^+\text{-N}$ and $\text{NO}_3^-\text{-N}$ concentrations in precipitation reflect the composition
277 of gaseous and particulate Nr species in the atmosphere (Celle-Jeanton et al., 2009;
278 Niu et al., 2014). Thus, the $\text{NH}_4^+\text{-N}/\text{NO}_3^-\text{-N}$ ratio in precipitation is a useful tool to
279 identify the predominant sources of N depositions in a targeted area (Xu et al., 2015).
280 It is widely agreed that a $\text{NH}_4^+\text{-N}/\text{NO}_3^-\text{-N}$ deposition ratio <1 within industrialized
281 regions and >1 within intensive agricultural regions (Xu et al., 2009). In the present
282 study, $\text{NH}_4^+\text{-N}/\text{NO}_3^-\text{-N}$ ratios in bulk deposition are greater than 1 at both the NC site
283 (average 1.70) and the SJL site (average 1.14), indicating that agricultural sources
284 (e.g., fertilized pastureland and farmland areas) dominate atmospheric N deposition in
285 the target area relative to industrial sources (e.g., transportation and combustion) . In
286 addition to local emission sources, long-range atmospheric transport of air mass also
287 has influences on N and/or P deposition at remote areas in Tibet (Liu et al., 2015; Xu
288 et al., 2017a). Based on the origin areas and transport directions, three and four
289 categories of air masses were identified from the entire set of trajectories at the NC
290 and SJL sites, respectively (Fig. 7). It is evident that the precipitation events during
291 the sampling period at both sites were dominated by air masses from the south region,
292 with the proportion of 65% and 62%, respectively. This is because southeast Tibet is
293 influenced by a southwest monsoon and the wind is mainly from the south (Yang et
294 al., 2012) where no heavy pollution sources are located. In addition, the
295 volume-weighted mean concentrations of DIN ($\text{NH}_4^+\text{-N}$ and $\text{NO}_3^-\text{-N}$), DON and TDP

296 in precipitation associated with two categories air masses (south and northwest) were
297 analyzed. As presented in Table 1, there were no large differences in concentrations
298 between the two directions. These results together to some extent suggest that
299 regional transport has little influences on N and P deposition at the two study sites,
300 which is more likely to be driven by local emission sources.

301 The chemical form of N input from the atmosphere plays a vital role in
302 regulating nutrient assimilation processes for plant growth in a wide variety of
303 ecosystems (Stevens et al., 2011; Harmens et al., 2014; Izquieta-Rojano et al., 2016).
304 Sheppard et al. (2014) demonstrated that NH_4^+ -N is more likely to be toxic to plant
305 root assimilation compared to NO_3^- -N. We found that NH_4^+ -N input was higher than
306 NO_3^- -N input, which might have potential harmful effects on local vegetation. Besides,
307 NH_4^+ -N deposition has a greater influence on vegetation composition compared to
308 NO_3^- -N deposition (van den Berg et al., 2016), since NH_4^+ -N deposition can lead to
309 soil acidification by release of H^+ ions (Du et al., 2015); being the main pathway of
310 biodiversity loss in ecosystems adapted to N-poor conditions (Boutin et al., 2015).
311 This could greatly affect biodiversity in subalpine coniferous forest and temperate
312 deciduous conifer mixed forest in southeast Tibet, which is recognized as a
313 biodiversity hotspot and is sensitive to elevated N deposition (You et al., 2013; Zhang
314 et al., 2014). Regarding the seasonal variation in bulk precipitation, the high NH_4^+ -N
315 and NO_3^- -N deposition fluxes in summer (June, July and August) could affect the
316 nutrient balance of N-poor ecosystems such as native fir forest (Edfast et al. 1990),
317 since this period is the vegetation growing season and deposited N can be absorbed by
318 vegetation in maximum degree. Earlier studies have demonstrated that an increase in
319 N deposition could result in a series of adverse effects on forest ecosystems, including
320 soil acidification (Bergkvist et al., 1992), ion leaching (Foster et al. 1989), increase of
321 leaf N concentration and photosynthetic rate (Magill et al. 2000; Nakji et al., 2001).

322 Atmospheric wet P deposition was on average $0.21 \text{ kg P ha}^{-1} \text{ yr}^{-1}$ (ranging from
323 0.002 to $2.53 \text{ kg P ha}^{-1} \text{ yr}^{-1}$) at 41 in situ observation sites across China and was 0.21
324 $\text{kg P ha}^{-1} \text{ yr}^{-1}$ on a global scale (Zhu et al., 2016; Tipping et al., 2014). At a point scale,
325 earlier studies based on field measurements demonstrated that bulk P deposition was

326 1.82 kg P ha⁻¹yr⁻¹ in Nanjing city (Sun et al., 2014), and wet P deposition was 0.9 kg P
327 ha⁻¹yr⁻¹ in Lake Taihu (Yang et al 2007). In the present study, bulk P deposition fluxes
328 were 0.58 and 0.68 kg P ha⁻¹ at the NC and SJL sites, respectively. Obviously,
329 estimated bulk P deposition in the study area was higher than the average levels in
330 China and in the world, but lower than those measured in southeast China.

331 Unbalanced human-induced N and P inputs to the atmosphere led to an increase
332 in the N/P ratio in wet/bulk deposition. Many studies has illustrated that the current
333 situation of N and P deposition shifts all over the world (Peñuelas et al. 2013;
334 Peñuelas et al., 2015). For example, foliar N concentrations from non-agricultural
335 ecosystems throughout China significantly increased from 1980 to 2000 in the context
336 of enhanced N deposition (Liu et al., 2013). It has been estimated that the N/P ratio in
337 bulk deposition was about 21.2 at a global scale and about 77 (based on mass) at a
338 national scale in China. At a regional scale, N/P ratios (based on mass) varied greatly
339 in different regions of China. For example, the N/P ratio was 10 in Yangzonghai (Yu
340 et al., 2017), 77 in Hangjiahu area (Wang et al., 2015), 30 in Nanjing city (Sun et al.,
341 2014), 14 in Taihu lake (Yang et al., 2007). Furthermore, due to enhanced N
342 deposition globally and intensified human activities in Tibet, Nr deposition is
343 expected to increase continuously in the future, which could promote plant growth
344 and further affect local plant community structure or phytocoenosis evolution.

345 **5. Conclusions**

346 The present study measured bulk deposition fluxes of DIN, DON and TDP at an
347 urban (NC) site and a forest (SJL) site in the southeast of the Tibetan Plateau during
348 the i main rainy seasons from March to October 2017. Total deposition of TDN and
349 TDP was 4.62 kg N ha⁻¹ yr⁻¹ and 0.68 kg P ha⁻¹ yr⁻¹ at SJL, and 3.57 kg N ha⁻¹ yr⁻¹ and
350 0.58 kg P ha⁻¹ yr⁻¹ at NC, respectively, with N/P ratios of 6.8 and 6.1. TDN and TDP
351 deposition fluxes were higher at SJL compared with those at NC, but the opposite
352 phenomenon was observed for TDN and TDP concentrations. At both o sites, DIN
353 deposition accounted for 65% and 62% of TIN deposition fluxes, with
354 NH₄⁺-N/NO₃⁻-N ratios greater than 1. In order to obtain systematic knowledge on the

355 sources, composition and rates of N and P deposition as well as its ecological effects,
356 additional monitoring sites, covering typical land use types in the region, should be
357 established in the future adopting standardized sampling protocols and analytical
358 methods.

359

360 **Acknowledgements**

361 This work was supported by Tibet Youth Science Foundation (2016ZR-NQ-09),
362 the National Key R&D Program of China (2017YFC0210106), and the National
363 Natural Science Foundation of China (41705130). The authors thank all members of
364 the National Field Scientific Observation Station of Alpine Forest Ecosystem for their
365 co-operation during this experiment.

366

367

368

369

370

371

372

373

374

375

376

377

378

379

380

381

382

383

384 **References**

- 385 Al-Khashman, O.A., 2009. Chemical characteristics of rainwater collected at a
386 western site of Jordan. *Atmos. Res.* 91, 53–61.
- 387 Bergkvist, B. O., Folkeson, L., 1992. Soil acidification and element fluxes of a *Fagus-*
388 *sylvatica*, forest as influenced by simulated nitrogen deposition. *Water Air Soil*
389 *Poll.* 65(1–2), 111–133.
- 390 Bertollini, T., Flechard, C.R., Fattore, F., Nicolini, G., Stefani, P., Materia, S.,
391 Valentini, R., Laurin, G.V., Castaldi, S., 2016. DRY and BULK atmospheric
392 nitrogen deposition to a West-African humid forest exposed to terrestrial and
393 oceanic sources. *Agric. For. Meteorol.* 218–219, 184–195.
- 394 Boutin, M., Lamaze, T., Couvidat, F., Pornon, A., 2015. Subalpine Pyrenees received
395 higher nitrogen deposition than predicted by EMEP and CHIMERE
396 chemistry-transport models. *Sci. Rep.* 5, 12942.
- 397 Bovallius, A., Bucht, B., Roffey, R., Anäs, P., 1978. Three-year investigation of the
398 natural airborne bacterial flora at four localities in Sweden. *Appl. Environ.*
399 *Microb.* 35(5), 847–52.
- 400 Calvo-Fernández, J., Marcos, E., Calvo, L., 2017. Bulk deposition of atmospheric
401 inorganic nitrogen in mountainous heathland ecosystems in north-western Spain.
402 *Atmos. Res.* 183, 237–244.
- 403 Celle-Jeanton, H., Travi, Y., Löye-Pilot, M.D., Huneau, F., Bertrand, G., 2009.
404 Rainwater chemistry at a Mediterranean inland station (Avignon, France): local
405 contribution versus long-range supply. *Atmos. Res.* 91, 118–126.
- 406 Draxler, R., Stunder, B., Rolph, G., Stein, A., Taylor, A., 2012. HYSPLIT4 user's
407 guide, version 4, report, NOAA, Silver Spring, MD.
- 408 Du, E., De Vries, W., Liu, X., Fang, J., Galloway, J.N., Jiang, Y., 2015. Spatial
409 boundary of urban 'acid islands' in southern China. *Sci. Rep.* 5:12625
- 410 Du, E.Z., De Vries, W., Han, W.X., Liu, X.J., Yan, Z.B., Jiang, Y., 2016. Imbalanced
411 phosphorus and nitrogen deposition in china's forests. *Atmos. Chem. Phys.*
412 16(13), 8571-8579.

413 Duce, R.A., Laroche, J., Altieri, K., Arrigo, K.R., Baker, A.R., Capone, D.G., Cornell,
414 S., Dentener, F., Galloway, J., Ganeshram, R.S., Geider, R. J., Jickells, T.,
415 Kuypers, M.M., Langlois, R., Liss, P.S., Liu, S.M., Middelburg, J.J., Moore,
416 C.M., Nickovic, S., Oschlies, A., Pedersen, T., Prospero, J., Schlitzer, R.,
417 Seitzinger, S., Sorensen, L.L., Uematsu, M., Ulloa, O., Voss, M., Ward, B.,
418 Zamora, L. 2008. Impacts of atmospheric anthropogenic nitrogen on the open
419 ocean. *Science* 320(5878), 893-897.

420 Edfast, A.B., Näsholm, T., Ericsson, A., 1990. Free amino acid concentrations in
421 needles of Norway spruce and scots pine trees on different sites in areas with two
422 levels of nitrogen deposition. *Can. J. Forest Res.* 20(8), 1132-1136.

423 Elser, J.J., Bracken, M.E.S., Cleland, E.E., Gruner, D.S., Harpole, W.S., Hillebrand,
424 H., Ngai, J.T., Seabloom, E.W., Shurin, J.B., Smith, J.E., 2007, Global analysis
425 of nitrogen and phosphorus limitation of primary producers in freshwater, marine
426 and terrestrial ecosystems, *Ecol. Lett.* 10(12), 1135–1142,

427 Foster, N.W., Hazlett, P.W., Nicolson, J.A., Morrison, I.K., 1989. Ion leaching from a
428 sugar maple forest in response to acidic deposition and nitrification. *Water Air
429 Soil Poll.* 48(1-2), 251-261.

430 Galloway, J.N., Dentener, F.J., Capone, D.G., Boyer, E.W., Howarth, R.W., Seitzinger,
431 S.P., Asner, G.P., Cleveland, C.C., Green, P.A., Holland, E.A., Karl, D.M.,
432 Michaels, A.F., Porter, J.H., Townsend, A.R., Vorosmarty, C.J., 2004. Nitrogen
433 cycles: past, present, and future. *Biogeochemistry* 70, 153-226.

434 Graedel, T.E., Hawkins, D.T., Claxton, L. D., 1986. Atmospheric Chemical
435 Compounds [M]. *Atmospheric Chemical Compounds*, 68(49):579–651.

436 Harmens, H., Schnyder, E., Thöni, L., Cooper, D.M., Mills, G., Leblond, S., Mohr, K.,
437 Poikolainen, J., Santamaría, J., Skudnik, M., Zechmeister, H.G., Lindroos, A.J.,
438 HanusIllnar, A., 2014. Relationship between site-specific nitrogen concentrations
439 in mosses and measured wet bulk atmospheric nitrogen deposition across Europe.
440 *Environ. Pollut.* 194, 50–59.

441 Hou, P.Q., Ren, Y.F., Zhang, Q.Q., Lu, F., Ouyang, Z.Y., Wang, X.K., 2012. Nitrogen
442 and phosphorous in atmospheric deposition and roof runoff. *Pol. J Environ. Stud.*

443 21(6), 1621-1627.

444 Izquieta-Rojano, S., García-Gómez, H., Aguiillaume, L., Santamaría, J.M., Tang, Y.S.,
445 Santamaría, C., Valiño, F., Lasheras, E., Alonso, R., Àvila, A., Cape, J.N.,
446 Elustondo, D., 2016. Throughfall and bulk deposition of dissolved organic
447 nitrogen to holm oak forests in the Iberian Peninsula: flux estimation and
448 identification of potential sources. *Environ. Pollut.* 210, 104–112.

449 Jia, Y.L., Yu, G.R., He, N.P., Zhan, X.Y., Fang, H.J., Sheng, W.P., Yao Z., Zhang D.Y.,
450 Wang Q.F., 2014. Spatial and decadal variations in inorganic nitrogen wet
451 deposition in china induced by human activity. *Sci. Rep.* 4(4), 3763.

452 Kuang, F.H., Liu, X.J., Zhu, B., Shen, J.L., Pan, Y.P., Su, M.M., Goulding K., 2016.
453 Wet and dry nitrogen deposition in the central Sichuan basin of china. *Atmos.*
454 *Environ.* 143, 39-50.

455 Liang, T., Tong, Y.A., Liu, X.J., Xu, W., Luo, X.S., Christie, P., 2016. High nitrogen
456 deposition in an agricultural ecosystem of Shanxi, china. *Environ. Sci. Pollut. R.*
457 23(13), 13210-13221.

458 Liu, J.Q., Zhang, Q.Q., Wu, W.S., Lin, W.Q., 1995. Analysis of pollen nutrition
459 components of *Dimocarpus longan*, *Territ. Nat. Resour. Stud.* 3, 73-73. (In
460 Chinese)

461 Liu, X.J., Duan, L., Mo, J.M., Du, E.Z., Shen, J.L., Lu, X.K., Zhang, Y., Zhou, X.B.,
462 He, C.N., Zhang, F.S., 2011. Nitrogen deposition and its ecological impact in
463 china: an overview. *Environ. Pollut.* 159(10), 2251.

464 Liu, X.J., Zhang, Y., Han, W.X., Tang, A.H., Shen, J.L., Cui, Z.L., Vitousek, P.,
465 Erisman, J.W., Goulding, K., Christie, P., Fangmeier, A., Zhang, F.S., 2013.
466 Enhanced nitrogen deposition over China. *Nature* 494, 459-462.

467 Liu, Y.W., Xu-Ri, Xu, X.L., Wei, D., Wang, Y.H., Wang, Y.S., 2013. Plant and soil
468 responses of an alpine steppe on the Tibetan Plateau to multi-level nitrogen
469 addition. *Plant Soil*, 373, 515– 529.

470 Liu, Y.W., Xu-Ri, Wang, Y.S., Pan, Y.P., Piao, S.L., 2015. Wet deposition of
471 atmospheric inorganic nitrogen at five remote sites in the Tibetan plateau. *Atmos.*
472 *Chem. Phys.* 15(20), 11683-11700.

473 Liu, Z.Y., Zhou, Y.J., Li, H., Han L. 2016. Variation Features of nitrogen deposition
474 fluxes in forest throughfall and its influencing factors in southeastern Tibet.
475 Meteor. Sci. Tech. 44 (10), 834-840. (In Chinese with English abstract)

476 Lü, C.Q., Tian, H.Q., 2007. Spatial and temporal patterns of nitrogen deposition in
477 china: synthesis of observational data. J Geophys. Res-Atmos. 112(D22),
478 229-238.

479 Lü, C.Q., Tian, H.Q., 2014. Half-century nitrogen deposition increase across china: a
480 gridded time-series data set for regional environmental assessments. Atmos.
481 Environ. 97, 68-74.

482 Luo, J., Wang, X.R., Yang, H., Yu, J.Z., Yang, L.Y., Qin, B.Q., 2011. Atmospheric
483 phosphorus in the northern part of Lake Taihu, china. Chemosphere 84(6),
484 785-791.

485 Ma, Z., Ma, M.J., Baskin, J.M., Baskin, C.C., Li, J.Y., Du, G.Z., 2014. Responses of
486 alpine meadow seed bank and vegetation to nine consecutive years of soil
487 fertilization. Ecol. Eng. 70(9), 92-101.

488 Magill, A.H., Aber, J.D., Berntson, G.M., McDowell, W.H., Nadelhoffer, K.J., Melillo,
489 J.M., 2000. Long-term nitrogen additions and nitrogen saturation in two
490 temperate forests. Ecosystems 3(3), 238-253.

491 Mahowald, N., Jickells, T.D., Baker, A.R., Artaxo, P., Benitez-Nelson, C.R.,
492 Bergametti, G., Bond T.C., Chen Y., Cohen, D.D., Herut, B., Kubilay, N., Losno,
493 R., Luo, C., Maenhaut, W., McGee, K.A., Okin, G.S., Siefert, R.L., Tsukuda, S.,
494 2008. Global distribution of atmospheric phosphorus sources, concentrations and
495 deposition rates, and anthropogenic impacts. Global Biogeochem. Cy. 22(4),
496 37-42.

497 Nakji, T., Fukami, M., Dokiya, Y., Izuta, T., 2001. Effects of high nitrogen load on
498 growth, photosynthesis and nutrient status of *cryptomeria japonica* and *pinus*
499 *densiflora* seedlings. Trees-Struct Funct. 15(8), 453-461.

500 Neff, J.C, Holland, E.A, Dentener, F.J, McDowell, W.H, Russell, K.M., 2002. The
501 origin, composition and rates of organic nitrogen deposition: A missing piece of
502 the nitrogen cycle? Biogeochemistry 57-58, 99-136.

503 Niu, H.W., He, Y.Q., Lu, X.X., Shen, J., Du, J.K., Zhang, T., Pu, T., Xin, H.J., Chang,
504 L., 2014. Chemical composition of rainwater in the Yulong Snow Mountain
505 region, southwestern China. *Atmos. Res.* 144, 195–206.

506 Parron, L.M., Bustamante, M.M.C., Markewitz, D., 2011. Fluxes of nitrogen and
507 phosphorus in a gallery forest in the Cerrado of central Brazil. *Biogeochemistry*
508 105(1–3), 89–104.

509 Peñuelas, J., Poulter, B., Sardans, J., Ciais, P., van der Velde, M., Bopp, L., Boucher,
510 O., Godderis, Y., Hinsinger, P. Llusia, J., Nardin, E., Vicca, S., Obersteiner, M.,
511 Janssens, I.A. 2013. Human-induced nitrogen–phosphorus imbalances alter
512 natural and managed ecosystems across the globe. *Nat Commun.* 4(1), 2934.

513 Peñuelas, J., Sardans, J., Rivas-Ubach, A., Janssens, I. A, 2012. The human - induced
514 imbalance between C, N and P in earth's life system. *Global Change Biol.* 18(1),
515 3–6.

516 Pineda Rojas, A.L., Venegas, L.E., 2010. Inter annual variability of estimated monthly
517 nitrogen deposition to coastal waters due to variations of atmospheric variables
518 model input. *Atmos. Res.* 96, 88–102.

519 Roy, A., Chatterjee, A., Tiwari, S., Sarkar, C., Das, S.K., Ghosh, S.K., Raha, S., 2016.
520 Precipitation chemistry over urban, rural and high altitude Himalayan stations in
521 eastern India. *Atmos. Res.* 181, 44–53.

522 Seinfeld J, Pandis S. *Atmospheric Chemistry and Physics*. New York: Wiley; 1998.

523 Smil, V., 2000, Phosphorus in the environment: Natural flows and human
524 interferences. *Annu. Rev. Energy Environ.* 25, 53–88.

525 Sheppard, L.J., Leith, I.D., Mizunuma, T., Leeson, S., Kivimaki, S., Cape, J.N., van
526 Dijk, N., Leaver, D., Sutton, M.A., Fowler, D., Van den Berg, L.J.L., Crossley, A.,
527 Field, C., Smart, S., 2014. Inertia in an ombrotrophic bog ecosystem in response
528 to 9 years' realistic perturbation by wet deposition of nitrogen, separated by form.
529 *Glob. Chang. Biol.* 20, 566–580. Stein, A.F., Draxler, R.R., Rolph, G.D., Stunder,
530 B.J.B., Cohen, M.D., Ngan, F., 2015. NOAA's HYSPLIT atmospheric transport
531 and dispersion modeling system. *Bull. Am. Meteorol. Soc.* 96 (12), 2059–2077

532 Stevens, C.J., Manning, P., Van den Berg, L.J.L., De Graaf, M.C.C., Wamelink,

533 G.W.W., Boxman, A.W., Bleeker, A., Vergeer, P., Arroniz-Crespo, M., Limpens,
534 J., Lamers, L.P.M., Bobbink, R., Dorland, E., 2011. Ecosystem responses to
535 reduced and oxidized nitrogen inputs in European terrestrial habitats. *Environ.*
536 *Pollut.* 159, 665–676.

537 Sun, L.Y, Liu, Y.L, Wang, J.Y, Khalil, M.A.K, Zou, J.W, Xiong, Z.Q., 2014.
538 Atmospheric nitrogen and phosphorus deposition at three sites in Nanjing, China,
539 and possible links to nitrogen deposition sources. *Clean-Soil Air Water* 42 (11),
540 1–10.

541 Tipping, E., Benham, S., Boyle, J.F., Crow, P., Davies, J., Fischer, U., Guyatt, H.,
542 Helliwell, R., Jacksonblake, L., Lawlor, A.J., Monteith, D.T., Rowe, E.C.,
543 Toberman, H., 2014. Atmospheric deposition of phosphorus to land and
544 freshwater. *Environ. Sci. Proc. Impacts* 16(7), 1608-1617.

545 Van den Berg, L.J.L., Jones, L., Sheppard, L.J., Smart, S.M., Bobbink, R., Dise, N.B.,
546 Ashmore, M.R., 2016. Evidence for differential effects of reduced and oxidized
547 nitrogen deposition on vegetation independent of nitrogen load. *Environ. Pollut.*
548 208, 890–897.

549 Xing, J.W., Song, J.M., Yuan, H.M., Li, X.G., Li, N., Duan, L.Q., Kang, X.M., Wang,
550 Q.D., 2017. Fluxes, seasonal patterns and sources of various nutrient species
551 (nitrogen, phosphorus and silicon) in atmospheric wet deposition and their
552 ecological effects on Jiaozuo bay, north china. *Sci Total Environ.* 576(576), 617.

553 Xu, W., Zheng, K., Liu, X.J., Meng, L.M., Huaitalla, R.M., Shen, J.L., Hartung E.,
554 Gallmann, E., Roelcke, M., Zhang F.S., 2014. Atmospheric NH₃ dynamics at a
555 typical pig farm in china and their implications. *Atmos. Pollut. Res.* 5(3),
556 455-463.

557 Xu, W., Luo, X.S., Pan, Y.P., Zhang, L., Tang, A.H., Shen, J.L., Zhang, Y., Li, K.H.,
558 Wu, Q.H., Yang, D.W., Zhang, Y.Y., Xue, J., Li, W.Q., Li, Q.Q., Tang, L., Lu,
559 S.H., Liang, T., Tong, Y.A., Liu, P., Zhang, Q., Xiong, Z.Q., Shi, X.J., Wu, L.H.,
560 Shi, W.Q., Tian, K., Zhong, X.H., Shi, K., Tang, Q.Y., Zhang, L.J., Huang, J.L.,
561 He, C.E., Kuang, F.H., Zhu, B., Liu, H., Jin, X., Xin, Y.J., Shi, X.K., Du, E.Z.,
562 Dore, A.J., Tang, S., Collett, J.L., Goulding, K., Sun, Y.X., Ren, J., Zhang, F. S.,

563 Liu, X. J., 2015. Quantifying atmospheric nitrogen deposition through a
564 nationwide monitoring network across china. *Atmos. Chem. Phys.* 15(21),
565 18365-18405.

566 Xu, W., Song, W., Zhang, Y.Y., Liu, X.J., Zhang, L., Zhao, Y.H., Liu, D.Y., Tang, A.H.,
567 Yang, D.W., Wang, D.D., Wen, Z., Pan, Y.P., Fowler, D., Collett Jr, J.L., Erisman,
568 J.W., Goulding, K., Li, Y., Zhang, F.S., 2017. Air quality improvement in a
569 megacity: implications from 2015 Beijing Parade Blue pollution control actions.
570 *Atmos. Chem. Phys.* 17 (1), 31-46.

571 Xu, W., Jin, X., Luo, X.H., Feng, Z.Z., Zhang, L., Pan, Y. P., Liu, X. J., 2017b. Dry
572 and bulk nitrogen deposition in suburbs of Xining City. *Environ. Sci.* 38(4),
573 1279-1288.

574 Xu, W., Zhao, Y.H., Liu, X.J., Dore, A.J., Zhang, L., Liu, L., Cheng, M.M., 2018.
575 Atmospheric nitrogen deposition in the Yangtze River basin: Spatial pattern and
576 source attribution. *Environ. Pollut.* 232, 546-555.

577 Xu, Z., Yan, X., Xiong, Z., Xie, Y., Xing, G., Shi, S., Zhu, Z., 2009. Spatial and
578 temporal variation of inorganic nitrogen wet deposition to the Yangtze River
579 delta region, china. *Water Air Soil Poll.* 203(1-4), 277-289.

580 Yang, L., Qin, B., Hu, W., Luo, L., Song, Y., 2007. The atmospheric deposition of
581 nitrogen and phosphorus nutrients in Taihu Lake. *Oceanologia Etlimnologia*
582 *Sinica.* 38(2):104-110. (In Chinese with English abstract).

583 Yang, R., Hayashi, K., Zhu, B., Li, F.Y., Yan, X.Y., 2010. Atmospheric NH₃ and NO₂
584 concentration and nitrogen deposition in an agricultural catchment of Eastern
585 China. *Sci. Total Environ.* 408, 4624-4632.

586 Yang X X, Xu B Q, Yang W, Qu D M., 2012. The Indian monsoonal influence on
587 altitude effect of $\delta^{18}\text{O}$ in surface water on southeast Tibetan Plateau. *Sci*
588 *China Earth Sci*, 55: 438–445.

589 You J., Feng J., 2013. Plant biodiversity and flora composition in Southeast Tibet.
590 *Ecol. Environ. Sci.* 22(2): 207-212. (In Chinese with English abstract).

591 Yu G.Y., Yang C.L., Yang C.L., Liu K., Yang H.Y., Zhang J.L., 2017. Atmospheric
592 deposition of nitrogen and phosphorous in Lake Yangzonghai, Yunnan Province.

593 J Lake Sci. 2017, 29(5):1134-1142. (In Chinese with English abstract)

594 Yu, W.T., Jiang, C.M., Ma, Q., Xu, Y.G., Zou, H., Zhang, S.C., 2011. Observation of
595 the nitrogen deposition in the lower liaohe river plain, northeast china and
596 assessing its ecological risk. Atmos. Res. 101(1), 460-468.

597 Zhang, Y. L., Li, B. Y., Zheng, D., 2002. A discussion on the boundary and area of the
598 Tibetan Plateau in China. Geographical Res., 21(1), 1–8, (in Chinese with
599 English abstract).

600 Zhang, Y., Song, L., Liu, X.J., Li, W.Q., Lü, S.H., Zheng, L.X., Bai, Z.C., Cai, G.Y.,
601 Zhang, F.S., 2012. Atmospheric organic nitrogen deposition in China. Atmos.
602 Environ. 46, 195–204.

603 Zhang, Y.H., Lu, X.T., Isbell, F., Stevens, C., Han, X., He, N.P, Zhang, G.M., Yu, Q.,
604 Huang, J.H., Han, X.G, 2014, Rapid plant species loss at high rates and at low
605 frequency of N addition in temperate steppe. Global Change Boil. 20(11):
606 3520-3529.

607 Zhu, J.X., He, N.P., Wang, Q.F., Yuan, G.F., Wen, D., Yu, G.R., Jia, Y.L., 2015. The
608 composition, spatial patterns, and influencing factors of atmospheric wet
609 nitrogen deposition in Chinese terrestrial ecosystems. Sci. Total Environ.
610 511(511), 777-785.

611 Zhu, J.X., Wang, Q.F., He, N.P., Smith, M.D., Elser, J.J., Du, J.Q., Yuan, G.F., Yu G.R.,
612 Yu, Q., 2016. Imbalanced atmospheric nitrogen and phosphorus depositions in
613 china: implications for nutrient limitation. J.Geophys. Res-Bioge. 121(6):1-12.

614 GB 11894-89, Water quality-Determination of total nitrogen-Alkaline potassium
615 persulfate digestion-UV spectrophotometric method. China national bureau of
616 technical supervision, 1989 (in Chinese).

617 GB 7479-87, Water quality-Determination of ammonia nitrogen-Nessler’s reagent
618 spectrophotometry. China national bureau of technical supervision, 1987 (in
619 Chinese).

620 GB 11893-89, Water quality-Determination of total phosphorus-Ammonium
621 molybdate spectrophotometric. China national bureau of technical supervision,
622 1989 (in Chinese).

623

624 **Figure captions**

625 Figure 1. Location of the two monitoring sites in Nyingchi city, southeast Tibet

626 Figure 2. Monthly precipitations and bulk deposition fluxes of N and P at the two
627 monitoring sites

628 Figure 3. Volume-weighted mean concentration of Nr species and P in precipitation

629 Figure 4. Correlations between precipitation and N deposition fluxes (a) and P
630 deposition fluxes (b) at the two sampling sites

631 Figure 5. Total N and P deposition fluxes during the observation period at the two
632 monitoring sites

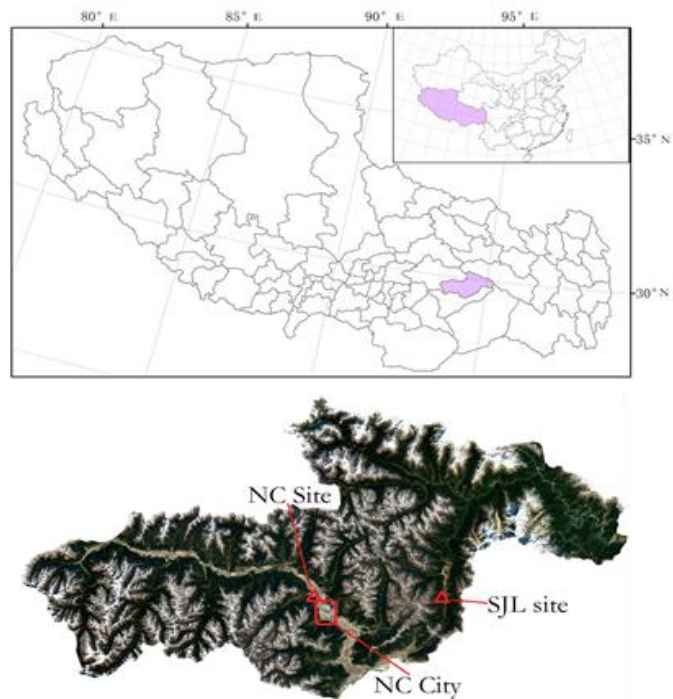
633 Figure 6. Correlation between concentrations of NO_3^- -N and NH_4^+ -N (a), between
634 concentrations of NO_3^- -N and DON (b) and concentrations of NH_4^+ -N and DON (c) at
635 the two sites

636 Figure 7. 3-day backward trajectories at NC (a) and SJL (b) sites in southeast Tibet.
637 Lines with different colors show the clustering trajectories.

638

639

640 **Figure 1**



641

642

643

644

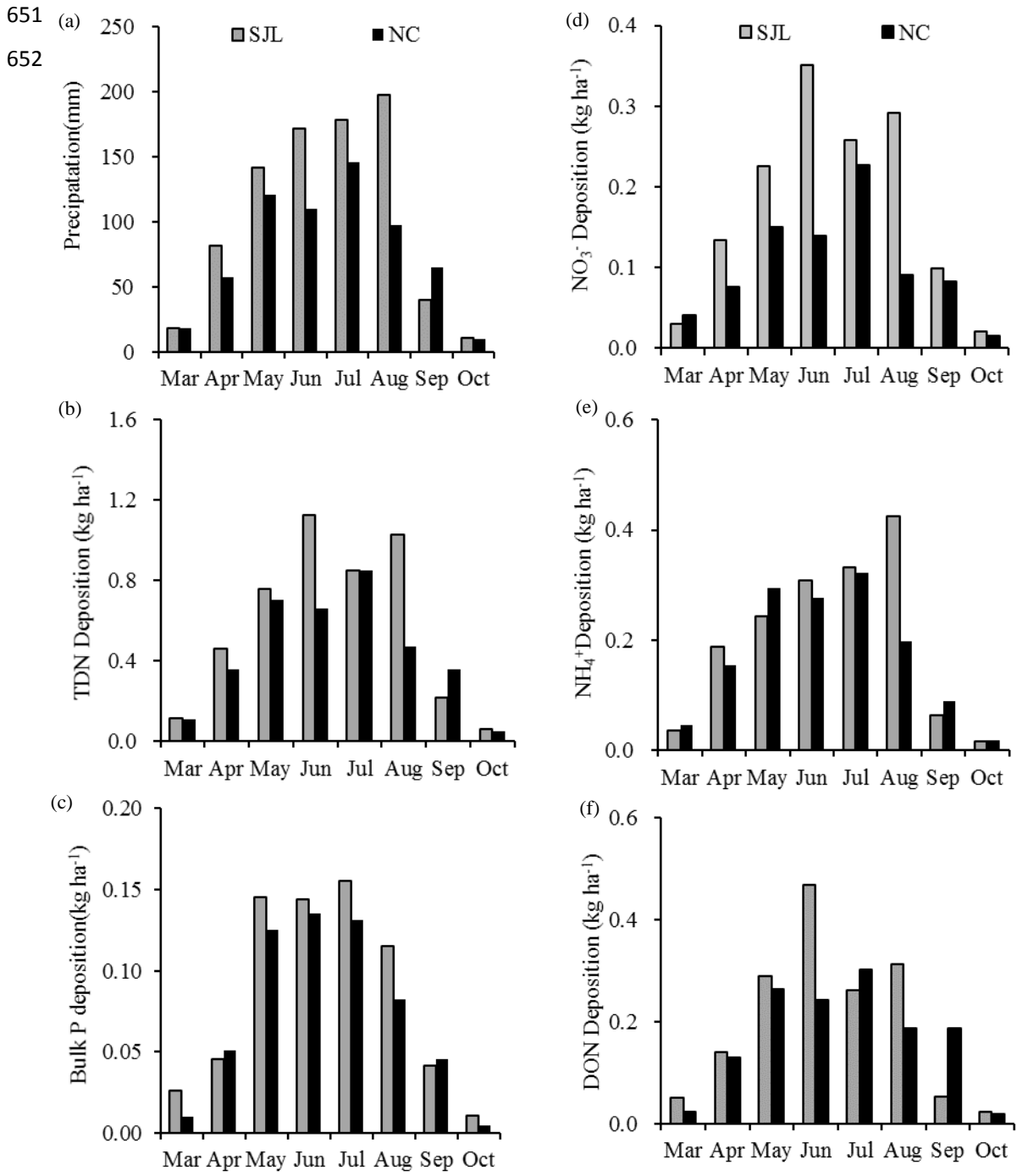
645

646

647

648

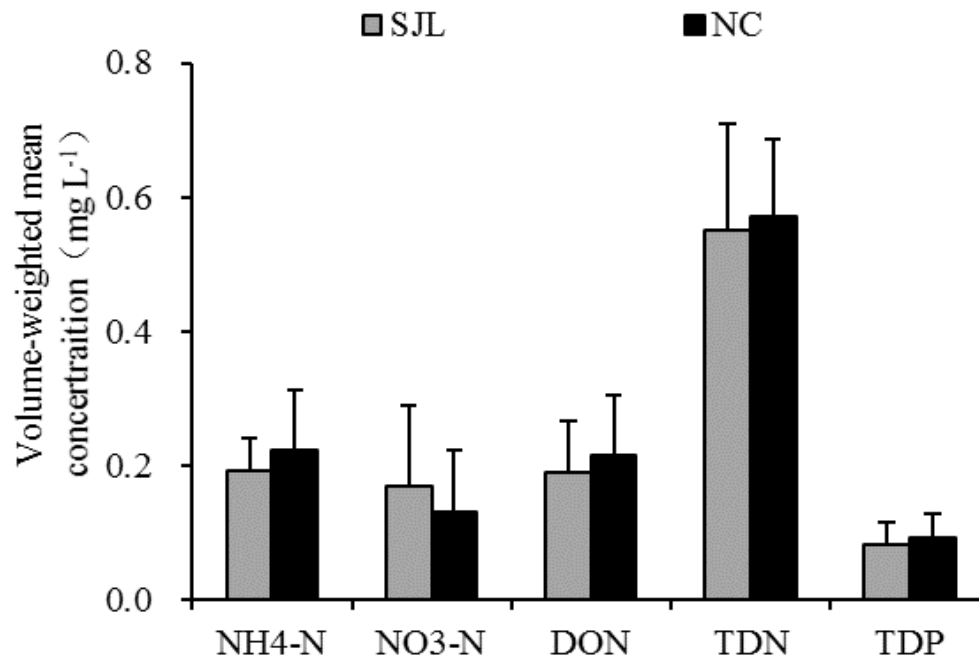
650 **Figure2**



653

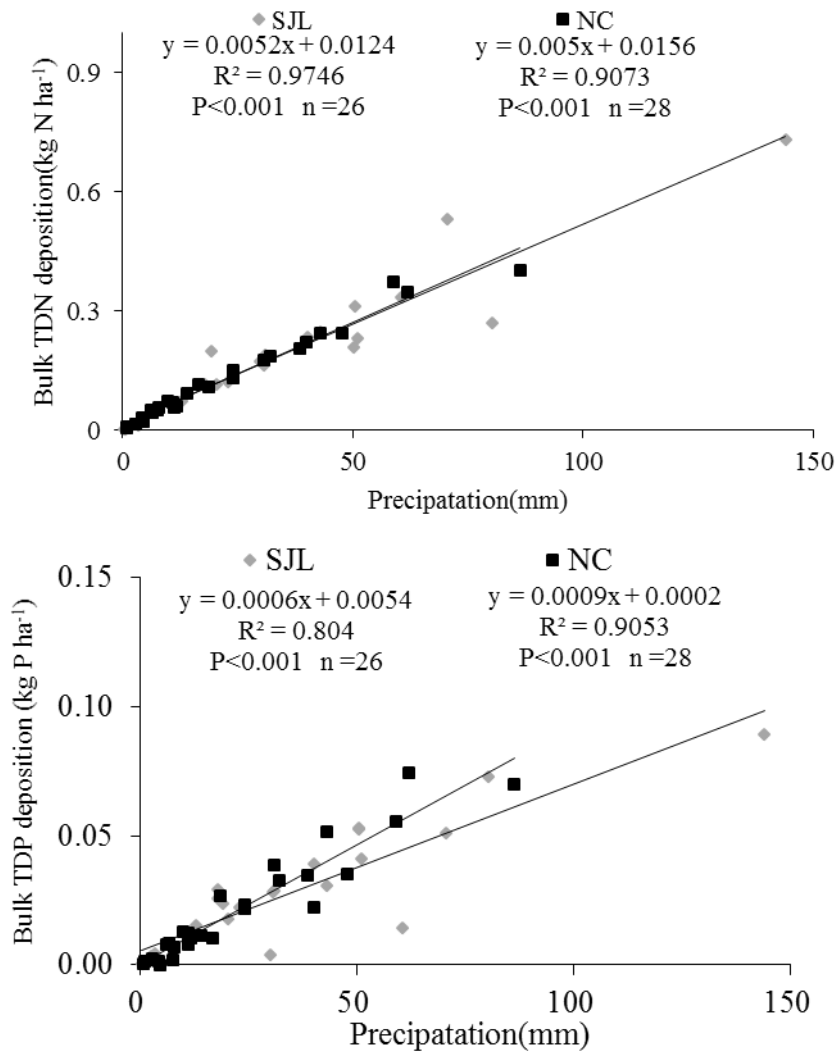
654 **Figure 3**

655



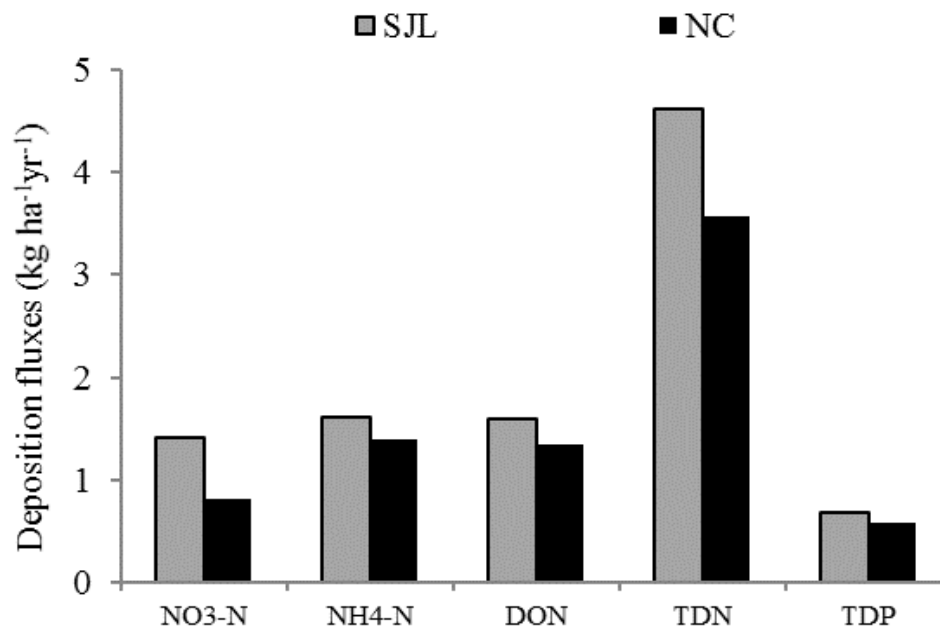
656

658 **Figure 4**



660

661 **Figure 5**

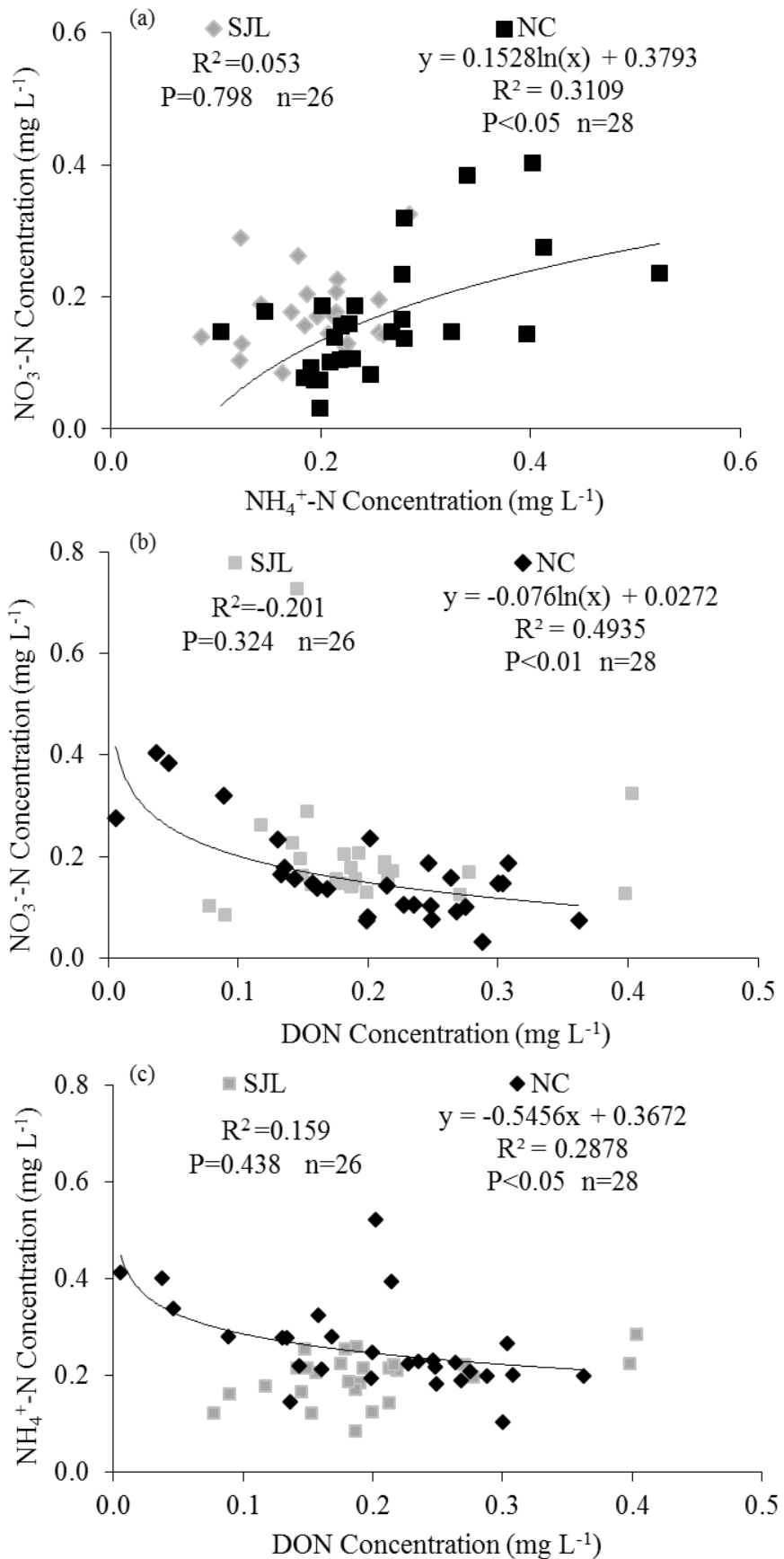


662

663

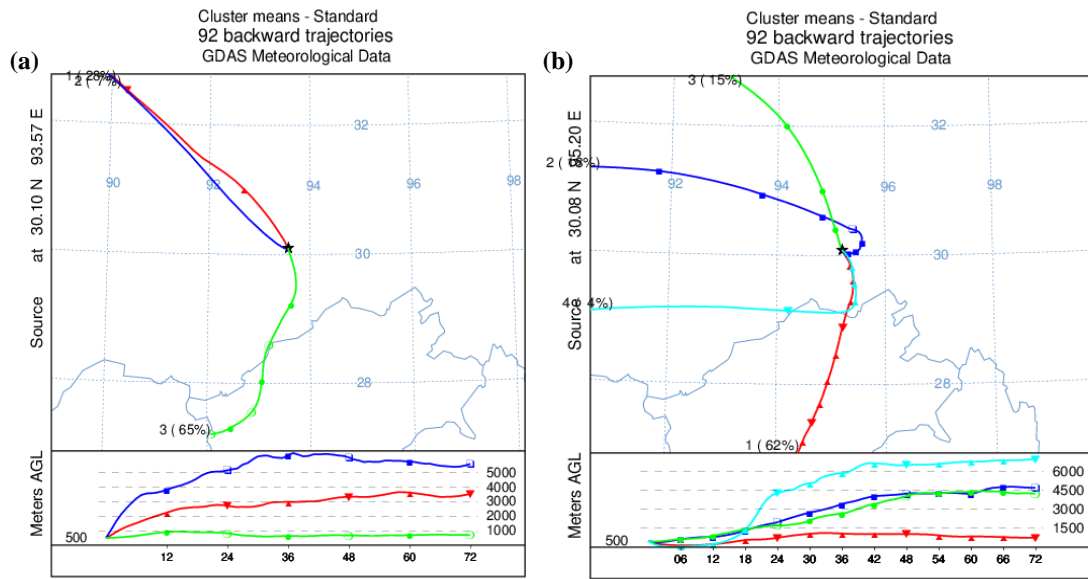
664 **Figure 6**

665



666

667 **Figure 7**



668

669

670

671

672

673

674

675

676

677

678

679

680

681

682

683

684

685

686

687

688

689

690

691

692

693

694

695

Table 1. Volume weight mean concentration (mg L⁻¹) in precipitation under the influences of two categories air masses

Site	Direction ^a	NO ₃ ⁻ -N	NH ₄ ⁺ -N	DON	TDN	TDP
NC	S	0.111	0.210	0.238	0.559	0.095
	NW	0.144	0.265	0.199	0.609	0.089
SJL	S	0.181	0.187	0.202	0.569	0.078
	NW	0.147	0.202	0.170	0.518	0.088

^a S: south; NW: northwest.